Image blind deblurring based on Laplacian gradients

Yue Han, Jiangming Kan[*]

Abstract—Image blind deblurring is an ill-posed inverse problem, in which the blurring kernel is unknown. In this paper, we propose a new image blind deblurring method. We introduce Laplacian operator to extract the gradients of the image instead of first- and second-order gradients, which simply the solving process. In the estimation framework, blurring kernel and image are alternately obtained. Compared with the state-of-the-art image deblurring methods, the image deblurred by the proposed method is more clearly and have higher fidelity, and the ringing artifacts are reduced effectively. From the image deblurring results, the kernel similarity of estimated blurring kernel is higher, the indices of image deblurring result are dominant as well.

Keywords—Image blind deblurring, ill-posed inverse problem image gradients, Laplacian operator.

I. INTRODUCTION

BLIND image deblurring is an ill-posed inverse problem, aiming at obtaining the clear image and blurring kernel from the blurred image. Images captured by cameras are often suffered from motion blur or out-of-focus blur, sometimes with additional noise, the process of image blur is modeled as:

$$B = H \otimes L + n \qquad (1)$$

Where B is the blurred image, H is the blurring kernel, L is the latent clear image, $\otimes$ is the convolution operator, n is the additional noise when capturing the image.

In non-blind image deblurring, H is known in advance, whereas in blind image deblurring, H and L are both need estimating. In image deblurring, clear image is estimated based on image deblurring model, and the edges or gradients of image are commonly utilized in the establishment of the image deblurring model. Total variation based image deblurring methods are widely used, which obtain the L2-norm of horizontal and vertical gradients [1]. However, the inaccurate estimation of image deblurring model in the classic total variation will lead to some problems, such as ringing artifacts [2]. In [3], a non-local self-similarity constraint is added in total variation term. In [4], Almeida et al. optimized the total variation term by introducing new edge detectors which add two directions on the basis of total variation regularization term. In addition to the first-order gradients, some researched introduce higher order gradients in the deblurring [2], and except for traditional higher order gradient operators, some researches introduce other regularizations, such as Hessian and affine TV function [5]. In [6], Cho et al. proposed the method to obtain image gradients by shock filter.

In other methods, new regularization terms are constructed by finding the distribution of image edges. In [2], Shan proposed the deblurring model by Bayes' theorem based on heavy-tailed distribution of image gradients, and the gradients of image are obtained by first-order gradient operators in horizontal and vertical directions; In [7], Javaran et al. found that the second-order gradients also have the heavy-tailed distribution and they add new regularization term in the deblurring model; In [8], Krishnan et al. proposed a Hiper-Laplacian model based on the research of heavy-tailed distribution, which found that the value of exponent $\alpha=2/3$ is the best model.

Gradients of images are considered as a vital factor in the establishing of deblurring model in the methods above, and the most commonly used gradient operators are the first- and second-order operators. However, adding too much operators will increase the computation, and traditional first- and second-order operators still have some drawbacks in the detecting of gradients.

The solving method of image and the blurring kernel is a challenging ill-posed problem, some methods estimate the

blurring kernel first and the image is then obtained by non-blind image deblurring methods [9], but the kernel estimated from this method is inaccurate, which will lead to the inaccurate estimating of image in return. Most blind image deblurring methods estimate image and kernel alternately from coarse to fine. Some objective functions of image deblurring model are convex, in order to solve this ill-posed inverse problem, Majorization-Minimization approach [1], Alternating direction method of multipliers (ADMM) [4] are used. The solving methods of non-convex problems includes FFT(Fast Fourier Transformation)[10], lookup-table(LUT) [8] and so on.

In the proposed method, we introduce Laplacian operator into the image deblurring model for its advantage in detecting the details of images. In order to avoid the existence of ringing artifacts, we set an image mask to establish a local constrain on the image. In the estimation process, the image and blurring kernel are alternately estimated. From the results of image deblurring, the proposed method are superior to the state-of-the-art methods, the kernel similarities are higher than others, and evaluate indices are all perform better.

II. METHOD

A. Image Deblurring Model

The image deblurring model in the proposed method is defined in (2), the local minimum values of L and H are the clear image and blurring kernel we aim to obtain.

$$E(L,H) = \left\| B - H \otimes L \right\|_2^2 + \left\| \Delta B - H \otimes \Delta L \right\|_2^2 + TV_{\text{local}} + \left\| H \right\|_p \quad (2)$$

In the proposed method, Lp-norm is used to make a constraint on the blurring kernel. Δ is the Laplacian operator, TV_{local} adds Laplacian operator based on total variation, which is shown in (3):

$$TV_{\text{local}} = \int_{\Omega} \sqrt{\partial_h L^2 + \partial_v L^2 + \Delta L^2} \quad (3)$$

∂_h is the first-order gradient operator in horizontal direction, and ∂_v is the first-order gradient operator in vertical direction. Ω is the image mask which varies with the changes of L.

To reserve the image boundaries, the input image in deblurring is processed by the boundary conditions (BCs) beforehand. To reduce the possible ringing artifacts caused by unsuitable boundary conditions, we use reflective BCs [11], which is defined in (4) and (5). The length of extended boundary is determined by the size of estimated kernel. Assume that the size of original image J is $m_0 \times n_0$, the size of blurring kernel is $h_1 \times h_2$ and I is the image processed with reflective BCs. $I_{[i,j]}$ is the pixel value in the location of $[i,j]$.

$$\begin{cases} I_{[1-i,j]} = J_{[i,j]} & i \le (h_1 - 1)/2 \\ I_{[m+i,j]} = J_{[m+1-i,j]} & i \ge (h_1 - 1)/2 + m_0 \end{cases} \quad (4)$$

$$\begin{cases} I_{[i,1-j]} = J_{[i,j]} & j \le (h_2 - 1)/2 \\ I_{[i,n+j]} = J_{[i,n+1-j]} & j \ge (h_2 - 1)/2 + n_0 \end{cases} \quad (5)$$

After obtaining the image I ($m \times n$) processed with reflective BCs, the first-order gradients are calculated as follows:

$$\partial_h I_{[i,j]} = \begin{cases} I_{[i+1,j]} - I_{[i,j]} & i \ne m \\ I_{[i,j]} & i = m \end{cases} \quad (6)$$

$$\partial_v I_{[i,j]} = \begin{cases} I_{[i,j+1]} - I_{[i,j]} & j \ne n \\ I_{[i,j]} & j = n \end{cases} \quad (7)$$

The gradient obtained by Laplacian is defined as follows:

$$\Delta I_{[i,j]} = \begin{cases} I_{[i+1,j]} + I_{[i-1,j]} + I_{[i,j+1]} \\ \qquad + I_{[i,j-1]} - 4I_{[i,j]} & i \ne 1, m \quad j \ne 1, n \\ I_{[i,j]} & i=1, m \quad j=1, n \end{cases} \quad (8)$$

B. Image Gradients and Local Constraint

Fig.1 shows different image gradients of the "barbara" image extracted by different gradient operators. From the comparison of different image gradients, the image gradients extracted by Laplacian operator include more details than other methods.

(a)   (b)   (c)

(d)   (e)   (f)
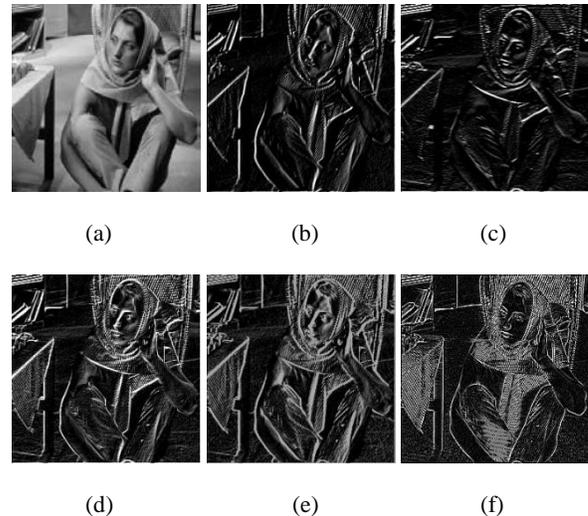
Fig.1 (a) "barbara" image; (b) image gradients in horizontal direction; (c) image gradients in vertical direction; (d) image gradients extracted by total variation method; (e) image gradients extracted by the method in [4]; (f) image gradients extracted by Laplacian operator

Although the details are more prominent using the Laplacian operator, side effects such as additional noise may occur, so an image mask is introduced to solve this problem in the proposed method. The method proposed in [2] uses the binary image as the image mask. In the proposed method, taking image structure into consideration, $r(x)$ is defined as follows:

$$r(x) = \frac{\left\| \Sigma_{\xi \in N(x)} \nabla_v B(\xi) \right\|}{\Sigma_{\xi \in N(x)} \left\| \nabla_v B(\xi) \right\| + 0.5} \tag{9}$$

$N(x)$ is window centered at pixel x, $r(x)$ reflects the usefulness of gradient at pixel x, and the larger value of $r(x)$ represents the stronger structure [10]. Then the image mask is defined as follows:

$$Mask(x) = \begin{cases} 1 & r(x) \geq \tau \\ 0 & r(x) < \tau \end{cases} \tag{10}$$

Where τ is the threshold. The image mask Ω in (3) is shown in Fig.2 (b), the pixel in white corresponds to 1, and the pixel in black corresponds to 0. The mask sets local constrain on TV_{local} norm. In the first several iterations, salient edges are detected, with the times of iteration increase, the details of image emerge gradually.

(a)   (b)
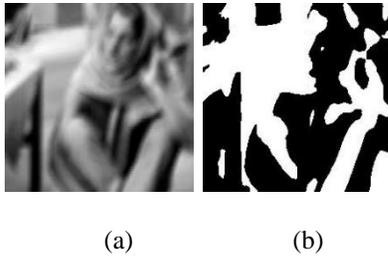
Fig.2 blurred image and the image mask

III. ESTIMATION FRAMWORK

A. Estimation of Blurring Kernel

The task of blurring kernel estimation is to obtain the minimum value of the cost function with regard to H, which is shown as follows:

$$\min_H \left\| B - H \otimes L \right\|_2^2 + \left\| \Delta B - H \otimes \Delta L \right\|_2^2 + \left\| H \right\|_p \tag{11}$$

When $p=1$, the value of H can be obtained from (12):

$$H = \frac{(1 + \Delta) \cdot \left(L^T \cdot B \right)}{(1 + \Delta) \cdot \left(L^T \cdot L \right) + 1} \tag{12}$$

L^T is the transposed matrix of L, when the image is transformed into frequency domain by Fourier transform, the multiplication operation will transformed into pixel-wise multiplication, and the solving of blurring kernel will be simplified.

When the value of p ranges from 0 to 1, then half-quadratic penalty method is used, then other variable is introduced to simplify the calculating. The solving of blurring kernel is shown in Algorithm 1. The variable δ_k (k=1, 2...15) in Algorithm 1 is calculated by Newton-Raphson method [8]. In the proposed method, the value of p in (11) is set to 0.8.

Algorithm 1. Solving of blurring kernel

---

1. Initialization: L, B, δ_0

2. **for** k=1:15

3. **repeat**

$$w_k = \frac{L^T \cdot B + \Delta L^T \cdot \Delta B + \delta_k}{L^T \cdot L + \Delta L^T \cdot \Delta L + 1}$$

$$\delta_k = \min_{\delta_k} | \delta_k |^p + (w_k - \delta_k)$$

4. **end**

5. H= w_{15}

B. Estimation of Image

The cost function of image L is shown in (13), and the local minimum of L is the clear image we aim to obtain.

$$\min_L \left\| B - H \otimes L \right\|_2^2 + \left\| \Delta B - H \otimes \Delta L \right\|_2^2$$
$$+ \int_\Omega \sqrt{\partial_h L^2 + \partial_v L^2 + \Delta L^2} \tag{13}$$

In our method, the image is estimated by Algorithm 2. In Algorithm 2, the problem of minimizing is calculated by soft threshold iterative method [12]. Soft threshold is utilized to solve the function as follows:

$$\min_P \left\| P - Q \right\|_2^2 / 2 + \lambda \left\| P \right\|_1 \tag{14}$$

The solution of (14) can be represented by

$$soft(Q,\lambda) = \begin{cases} Q + \lambda & Q < -\lambda \\ 0 & |Q| < \lambda \\ Q - \lambda & Q > \lambda \end{cases} \quad (15)$$

Algorithm 2. Solving of image

---

1. Initialization: $z_1 = L$; a_0, b_0, c_0; $\Theta \in \{\partial_h, \partial_v, \Delta\}$

2. **for** k=1:15

3. **repeat**

$$a_{k+1} = \int_{\Omega} \sum_{\partial_* \in \Theta} (\partial_*)^T \cdot [a_k - \partial_* z_{k+1}$$
$$+ \arg\min_{z_{k+1}} (\|\partial_* z_{k+1} - a_k - z_k\| + \|z_k\|)]$$

$$b_{k+1} = (H)^T \cdot [b_k - \Delta z_{k+1}$$
$$+ 2\arg\min_{z_{k+1}} (\|\Delta z_{k+1} - b_k - z_k\| + 2\|z_k\|)]$$

$$c_{k+1} = (H)^T \cdot c_k - z_{k+1}$$
$$+ 2\arg\min_{z_{k+1}} (\|z_{k+1} - c_k - z_k\| + 2\|z_k\|)$$

$$z_{k+1} = \frac{a_{k+1} + b_{k+1} + c_{k+1}}{\sum_{\Theta} (\partial_*)^T \cdot (\partial_*) + 2(H)^T \cdot (H)}$$

4. **end**

5. $L = z_{15}$

C. Iteration procedure

In blind deblurring, the only variation we know is the blurred image, which is set as the initial value of image *L*. In the first iteration, only weak assumption of the kernel is built and strong edges of image are detected, as the estimation process going on, and the kernel are closer to the real blurring condition. The flowchart of the proposed method is in Fig.3.
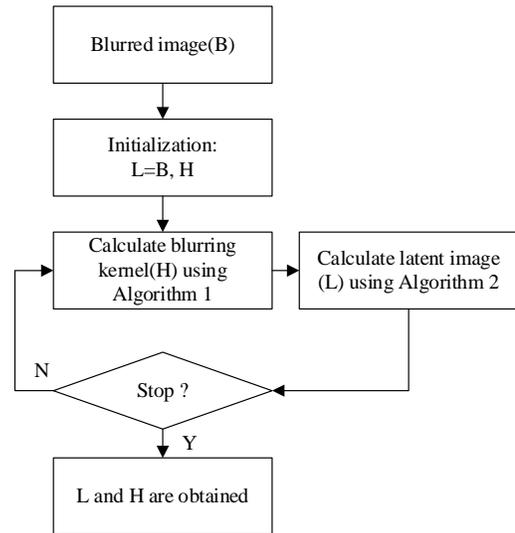
Fig.3 the flowchart of proposed method

The stopping criterion in the proposed method is based on PSNR (peak signal-to-noise ratio), PSNR is defined as follows:

$$PSNR = 10\log_{10} \frac{255^2}{MSE} \quad (16)$$

MSE is the mean square error, which is defined as follows:

$$MSE = \frac{1}{M \times N} \sum_{i=1}^{M} \sum_{j=1}^{N} \left(L_{[i,j]} - B_{[i,j]} \right) \quad (17)$$

Where *M* is the length of the image and *N* is the width of the image. With the iteration numbers increase, the PSNR of the image gradually increase and then decrease. We stop the iteration when PSNR reaches to the peak value. In the proposed method, when PSNR starts decreasing, we consider that the PSNR has reached the peak value, the iteration should be stopped, and we obtain the final results of image and kernel corresponding to the peak value of PSNR.

In the iteration procedure, the changes of image and kernel with the increasing of iteration numbers are shown in Fig.4 and Fig.5.

(a)   (b)   (c)

(d)	(e)	(f)
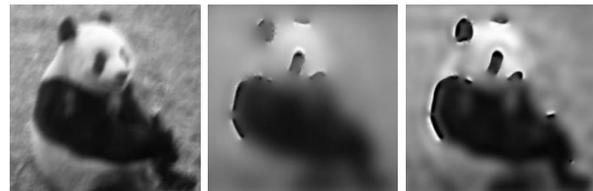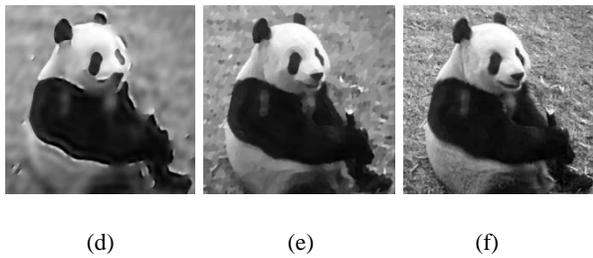
Fig.4 the image estimation in the solving process:(a) blurred image; (b) result in the 1st iteration; (c)result in the 3rd iteration; (d) result in the 6th iteration; (e)result in the 9th iteration; (f)final estimated image

(a)	(b)	(c)	(d)	(e)
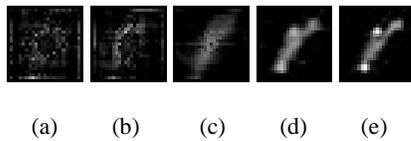
Fig.5 the kernel estimation in the solving process: (a) result in the 1st iteration; (b)result in the 3rd iteration; (c) result in the 6th iteration; (d)result in the 9th iteration; (e) final estimated kernel

IV. RESULT

A. Results of kernel estimation

In our experiment, the blurred images are established based on the dataset of Levin [13]. Fig.6 shows the kernel estimating results of the proposed method and the method proposed by Shan et al. [2], method proposed by Krishnan et al. [9], and the method proposed by Xu et al. [10]. The results show that our method estimates blurring kernel better.

(a)

(b)

(c)

(d)
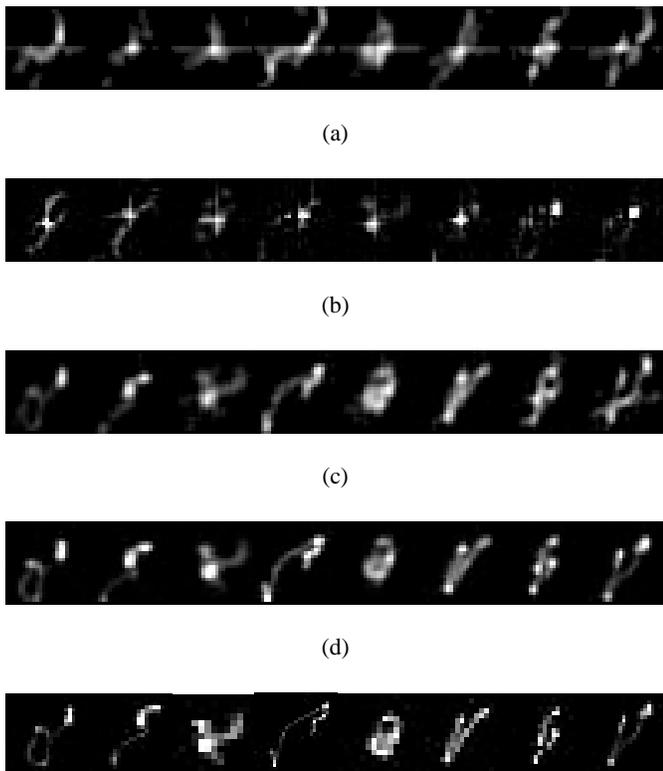
(e)

Fig.6 estimated kernel comparison: (a) estimated kernel by Shan et al.; (b) estimated kernel by Krishnan et al.; (c) estimated kernel by Xu et al.; (d) estimated kernel by proposed method; (e) real kernel

To evaluate the estimation accuracy, we compare the kernel similarity with other methods, the results are shown in Fig.7. The kernel similarity of the proposed method is 6.16% higher than the method of Shan et al., 7.83% higher than the method of Krishnan et al., and 6.03% higher than the method of Xu et al. averagely.
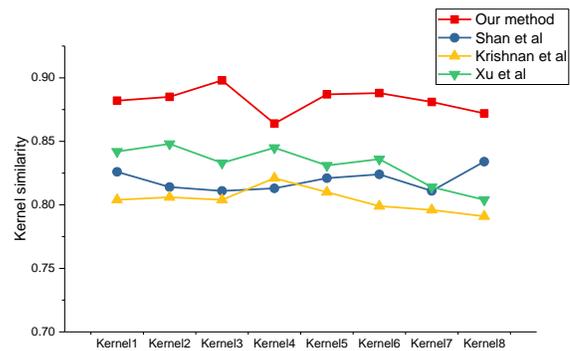
Fig.7 comparison of kernel similarity

B. Results of image estimation

Experimental results also show that the image estimated by our method is more clearly and have higher fidelity. We compare the proposed method with the methods in [2], [9],[10] and in the non-blind deblurring method in [8], the blurred images are obtained by the kernels in Fig.6(e). The results show that our method performs better not only than the blind deblurring methods, but also better than non-blind deblurring method.
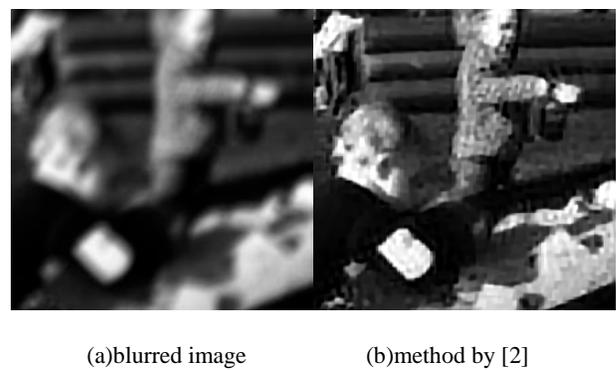
(a)blurred image	(b)method by [2]

(c) method by [8]   (d) method by [9]

(e)method by [10]   (f) proposed method

Fig.9 image deblurring comparison

(e) method by [10]   (f) proposed method

Fig.8 image deblurring comparison

As Fig.9 shows, images deblurred by the proposed method overcome the problem of ringing artifacts, and the edges of image obtained by the proposed method are stronger, more detailed information can be obtained from the image.

To evaluate the deblurring results, except for the images shown above, we deblur other two images by the proposed method and other methods. The evaluation indices include SSIM [14], MS-SSIM [15], and IFC [16]. SSIM (structural similarity) measures the similarity between the real clear image and the deblurred image. The higher value of SSIM, the image deblurred by the method is better. MS-SSIM (multi-scale structural similarity) is introduced based on the SSIM, in which the visual characteristics are considered. Higher value of MS-SSIM reflects better performance of the method. IFC is an information fidelity criterion, and the higher value of IFC represents better fidelity. When same index by different deblurring methods is calculated, the calculating steps are consistent, and for the sake of comparison, all the indices are normalized.

(a)blurred image   (b)method by [2]

(c)method by [8]   (d) method by [9]

Table 1. Comparison of SSIM

	Method by [2]	Method by [8]	Method by [9]	Method by [10]	Proposed method
Children	0.782	0.816	0.788	0.806	**0.824**
Castle	0.796	0.805	0.825	0.831	**0.840**
Flower	0.824	**0.832**	0.822	0.822	0.827
Panda	0.813	0.822	0.801	0.826	**0.836**

Table 2. Comparison of MS-SSIM

	Method by [2]	Method by [8]	Method by [9]	Method by [10]	Proposed method
Children	0.796	0.812	0.788	0.811	**0.852**
Castle	0.801	0.820	0.796	0.804	**0.835**

Flower	0.804	0.812	0.822	0.801	**0.837**
Panda	0.792	0.800	0.813	0.817	**0.842**

Table 3. Comparison of IFC

	Method by [2]	Method by [8]	Method by [9]	Method by [10]	Proposed method
Children	0.900	0.862	0.858	0.884	**0.902**
Castle	0.904	0.884	0.879	0.891	**0.913**
Flower	0.872	0.877	0.870	0.876	**0.899**
Panda	0.897	0.901	0.881	0.887	**0.906**

V. CONCLUSION

In this paper, a blind deblurring method based on Laplacian operator is proposed. In the image deblurring model, we use Laplacian operator instead of traditional operators. In image estimating, an image mask is set to establish a local constrain on the image, and in kernel estimating, Lp-norm of the kernel is set to make a constraint. The image and blurring kernel are alternately estimated in solving framework.

Compared with the state-of-the-art methods, image deblurred by our method perform better in image details and fidelity. The kernel similarity, SSIM, MS-SSIM and IFC of our methods are all dominant among the methods we test in experiment.

REFERENCES

[1]Oliveira J P, Bioucas-Dias J M, Figueiredo M A T. Adaptive total variation image deblurring: A majorization-minimization approach [J]. Signal Processing. 2009, 89(9): 1683-1693.

[2]Shan Q, Jia J, Agarwala A. High-quality motion deblurring from a single image [J]. ACM Transactions on Graphics. 2008, 27(733).

[3]Wang S, Liu Z W, Dong W S, et al. Total variation based image deblurring with nonlocal self-similarity constraint [J]. Electronics Letters. 2011, 47(16): 916-918.

[4]Almeida M S C, Almeida L B. Blind and Semi-Blind Deblurring of Natural Images [J]. IEEE Transactions on Image Processing. 2010, 19(1): 36-52.

[5]Lefkimmiatis S, Bourquard A, Unser M. Hessian-Based Norm Regularization for Image Restoration With Biomedical Applications [J]. IEEE Transactions on Image Processing. 2012, 21(3): 983-995.

[6]Cho S, Lee S. Fast Motion Deblurring [J]. ACM Transactions on Graphics. 2009, 28(1455).

[7]Javaran T A, Hassanpour H, Abolghasemi V. Local motion deblurring using an effective image prior based on both the first- and second-order gradients [J]. Machine Vision and Applications. 2017, 28(3-4): 431-444.

[8]Krishnan D, Fergus R. Fast image deconvolution using hyper-Laplacian priors. In NIPS[C]// Advances in Neural Information Processing Systems 22: Conference on Neural Information Processing Systems 2009. Proceedings of A Meeting Held 7-10 December 2009, Vancouver, British Columbia, Canada. DBLP, 2009:1033-1041.

[9]Krishnan D, Tay T, Fergus R. Blind deconvolution using a normalized sparsity measure[C]. IEEE Conference on Computer Vision and Pattern Recognition. IEEE Computer Society, 2011:233-240.

[10]Xu L, Jia J. Two-Phase Kernel Estimation for Robust Motion Deblurring[C]. Computer Vision - ECCV 2010, European Conference on Computer Vision, Heraklion, Crete, Greece, September 5-11, 2010, Proceedings. DBLP, 2010:157-170.

[11]Donatelli M, Serra-Capizzano S. Anti-reflective boundary conditions and re-blurring [J]. Inverse Problems. 2005, 21(1): 169-182.

[12]WrightS J, Nowak R D, Figueiredo M A T. Sparse reconstruction by separable approximation [J]. IEEE Transactions on Signal Processing, 2009,57(7):3373-3376.

[13]Levin A, Weiss Y, Durand F, et al. Understanding and evaluating blind deconvolution algorithms [J]. CVPR, IEEE Computer Society Conference on Computer Vision and Pattern Recognition. IEEE Computer Society Conference on Computer Vision and Pattern Recognition 2009, 8 (1) :1964-1971.

[14]Wang Z, Bovik AC, Sheikh H R, Simoncelli E P. Image quality assessment: from error visibility to structural similarity [J]. IEEE Transactions on Image Processing, 2004 , 13 (4) :600-612.

[15]Wang Z, Simoncelli E P, Bovik AC. Multiscale structural similarity for image quality assessment [J]. Conference on Signals, Systems & Computers 2003 , 2 (2) :1398-1402.

[16] Sheikh H R, Bovik A C, Veciana G D. An information fidelity criterion for image quality assessment using natural scene statistics [J]. IEEE Transactions on Image Processing, 2005, 14 (12):2117-2128.